Statistical Petrology Reveals a Link Between Supercontinents Cycle and Mantle Global Climate

Jérôme Ganne[1] , Xiaojun Feng[1], Patrice Rey[2], Vincent De Andrade[3]

1 - IRD, UR 234, GET, Université Toulouse III, 14 Avenue Edouard Belin, 31400 Toulouse, France

2 - Earthbyte Research Group, School of Geosciences, The University of Sydney, Sydney NSW 2006, Australia

3- Argonne National Laboratory, 9700 S. Cass Avenue, Argonne, IL 60439, Chicago, USA

ABSTRACT - The breakup of supercontinents is accompanied by the emplacement of continental flood basalts and dyke swarms, the origin of which is often attributed to mantle plumes. However, convection modeling has showed that the formation of supercontinents result in the warming of the sub-continental asthenospheric mantle (SCAM), which could also explain syn-breakup volcanism. Temperature variations during the formation then breakup of supercontinents are therefore fundamental to understand volcanism related to supercontinent cycles. Magmatic minerals record the thermal state of their magmatic sources. Here we present a data mining analysis on the first global compilation of chemical information on magmatic rocks and minerals formed over the past 600 million years; a time period spanning the aggregation and breakup of Pangea, the last supercontinent. We show that following a period of increasingly hotter Mg-rich magmatism with dominant tholeiitic affinity during the aggregation of Pangea, lower-temperature minerals crystallized within Mg-poorer magma with a dominant calc-alkaline affinity during Pangea disassembly. These trends reflect temporal changes in global mantle climate and global plate tectonics in response to continental masses assembly and dispersal. We also show that the final amalgamation

of Pangea at ~300 Myr led to a long period of lithospheric collapse and cooling until the major step of Pangea disassembly started at ~125 Myr. The geological control on the geosphere magma budget has implications on the oxidation state and temperature of the Earth's outer envelopes in the Phanerozoic and may have exerted indirect influence on the evolution of climate and life on Earth.

INTRODUCTION

Mantle convection and plate tectonics are two coupled processes driving the cooling of the Earth's interior (Labrosse and Jaupart, 2007). In the last decade, numerical studies have shown that the distribution and size of continental plates at the Earth surface control the mantle potential temperature (*Tp*) below continents (Gurnis, 1988; Yale and Carpenter, 1998; Grigné et al., 2005; Phillips and Bunge, 2005). The concept of mantle warming below supercontinents (Anderson, 1982; Coltice et al., 2009) has challenged the plume paradigm (Hill, 1991; Ernst and Buchan, 1997; Courtillot et al., 1999) to explain continental flood basalts (CFBs) and their dyke swarms which are now group as Large Igneous Provinces (LIPs) (Ernst, 2014). Two- and three-dimensional numerical studies (Gurnis, 1988; Grigné et al., 2005; Coltice et al., 2007; Lénardic et al., 2011) show that the potential temperature of the convective mantle gradually increases up to ~150 °C as a response of the lengthening of the convective wavelength as plates aggregate into a supercontinent. Locally, this seems to be confirmed as primary magmas from the ~200 Myr old Central Atlantic Magmatic Province (CAMP), emplaced at the onset of Pangea dispersal, point to a *Tp* 50 to 150 ºC warmer than normal, but not warm enough for a plume origin according to some authors (Hole, 2015; Rey, 2015). However, it remains quite uncertain how great an excess Tp might be derived from a plume originating from the deep mantle (Bunge, 2005). Though, if the supercontinent cycle modulates the temperature in the convective mantle then, on a global scale, magmatic minerals like olivine, pyroxene, amphibole and plagioclase should have recorded over the past ~600 Myr a measurable increase in crystallization temperature (*T*) in relation to the Pangea assembly phase, and decrease during its dispersal.

Despite uncertainties in measuring absolute values of *T* and *Tp* (Herzberg, 2011; Putirka, 2016), we hypothesize that their trends over several tens to hundreds Myrs are likely to be representative of changing thermal regimes in the sub-continental asthenospheric mantle (SCAM). **Figure 1a** illustrates how the melting temperature at the solidus, described by the potential temperature, impacts the chemical signature (MgO content) of magmas formed at the solidus (i.e. primary magmas). During mantle upwelling, including that induced by thinning of the continental lithosphere, the “exhumed “ mantle follows an adiabat (blue or red dashed lines) intersecting the solidus at a depth which depends on the potential temperature (blue and red dots in **Fig.1a**). Primary melts are produced between the solidus where melting begins (blue and red stars in **Fig.1a**) and the base of the lithosphere where melting ceases. This is called decompression melting. Melting is fractional, and the primary melt is the average of the melt compositions that are generated between the pressures at which melting begins and ends. Should these melts be extracted as soon as they are produced, they would follow their respective melt adiabat (black arrows). During fast ascent through a thin and/or hot continental lithosphere, the composition of basaltic magmas reaching the Earth’s surface remains largely unchanged (Putirka, 2008). As the magmas approach the surface, olivine crystallizes within a few 10’s of km from the surface (Ghiorsio & Sack, 1995). The potential temperature of the mantle, from which these olivine-bearing tholeiitic basalts are extracted, can be derived from the composition of the olivine (Putirka, 2016). In contrast, during slow ascent through a thick and/or cooler continental lithosphere, sequential crystallization and separation of minerals causes basaltic melts to evolve toward a progressively more calc-alkaline, Si-rich, composition (Grove and Baker, 1984), especially if water is present. If the starting basalt was not sufficiently hydrous, fractional crystallization will likely lead to alkaline, not calc-alkaline differentiation. Importantly, clinopyroxene and plagioclase start to crystallize earlier and at higher-pressure than olivine (Grove and Baker, 1984; Ghiorsio & Sack, 1995; Villiger et al, 2007; Whitaker et al., 2007; Smith, 2014). As MgO is incorporated into the clinopyroxene, the residual melt in calc-alkaline basalts tends to have a lower MgO content. In addition, as pressure (and water) promotes the incorporation of Ca in plagioclase, basaltic melts become depleted in Ca as they approach the surface. Continued fractionation at lower pressure leads to magmatic rocks of dacitic and rhyolitic composition (Bachmann, 2016). These first order petro-geochemical rules suggest that magmatic systems characterized by low level of fractionation, in the near absence of water, can potentially capture changing thermal regimes in the sub-continental asthenospheric mantle (SCAM), whereas in fractionated and more hydous (i.e. calc-alkaline) magma systems the complementary compositional trends of pyroxene and feldspar can give insights into the thermal and hydrous state and/or thickness of the lithosphere.

METHOD

Following the methods of Putirka (2008), built on a comprehensive review of thermo-barometers for magmatic rocks, we compared different magmatic mineral compositions with bulk rock compositions using experimentally derived thermometers to obtain temperatures of crystallization. To unravel the thermal evolution of magmas we have used only the most robust thermometers as proposed in Putirka (2008) and Ridolfi and Renzulli (2012). While magmatic temperatures can be confidently calculated from many silicate minerals in equilibrium with its hosting magma (Putirka, 2008), the calculation of pressure suffers larger uncertainties and was not considered here. To estimate global magmatic temperature and map its trend over the past 600 Myr, we compiled from GEOROC a database including over 16 million data points derived from geo-referenced bulk-rock composition (dominantly volcanic) and associated mineral analysis (see **Methods** in the supplementary material). The evolution of global mean intensive (geochemical) and extensive (*T*, *Tp*) parameters is reported with associated 1-standard-error of the sample mean at 50 Myr intervals. These means were generated by Monte Carlo analysis with bootstrap resampling techniques to mitigate sampling bias (Keller and Schoene, 2012). A polynomial curve (N, R^2) fitting the bootstrapped values was reported on the graphs. Data mining on large geochemical datasets gives access to global trends by integrating much of the high-frequency variations and complex details that can exist in magmatic systems. However, because contrasting trends can reflect contrasting tectono-magmatic systems we have organized our data into three groups according to the inferred tectonic environment proposed by the authors of data referenced in GEOROC. These three groups are (1) continental margins, (2) intra-continental settings (CFBs, LIPs, rift-related magmatism and intraplate volcanism, including syn- to post orogenic magmatism) and (3) oceanic domains. By considering the broad tectonic setting of all samples we can explore their temporal relationship with respect to the timing of amalgamation and disassembly of Pangea.

RESULTS

The temporal distribution of magmatic rocks and minerals is documented in **Fig. 1 and 2** and in the supplementary material (**SI Fig. 1 to 18**). The oceanic record is missing prior to 250 Myr (**Fig. 1b***)* due to seafloor recycling through subduction during Pangea amalgamation. It progressively increases after ~250 Myr as predicted by seafloor spreading accompanying Pangea dispersal. Conversely, arc-magmatism at continental-margins decreases from 600 to ~250 Myr, before increasing again in the last ~200 Myr (**Fig. 1b**). This pattern is consistent with the expected decrease in the number of subduction zones during Pangea assembly as continental blocks get sutured, from 460 to 275 Myr ago, along a global network of orogenic belts (e.g. Appalachian, Caledonian, Alleghanian, Variscan, Mauritanides, Ural Mountains). This global tectonic trend predicts and explains the observed global magmatic transition from dominant calc-alkaline signature (**Fig. 1c** and **SI Fig. 11 & 12**) characterizing arc magmatism (Chiaradia, 2014), to dominant tholeiitic composition between ~300 Myr and ~200 Myr when Pangea was stable. The increase in the continental record of calc-alkaline magmas after ~200 Myr can be linked to the initiation, during Pangea dispersal, of many subduction zones promoting fractional crystallization in the deep crust of hydrous arc magmas (Chiaradia, 2014), and increasing contribution of shallow and more differentiated magma sources from continental reworking (magma mixing, Grove and Baker, 1984). Moreover, one highly efficient category of continental reworking, that is too often overlooked, is via sediment subduction and subduction erosion - whereby subducted material of continental crustal origin is subducted and incorporated directly into new magmas. If these mechanisms are important for crustal reworking, this would produce a strong positive correlation between calc-alkaline magmatism and crustal reworking.

Continental reworking is recorded in the geochemical signature of magmatic biotite (Shabani et al., 2003) forming at supra-subduction or crustal levels, with a transition from metaluminous (mantle-derived I-type granitoids) to peraluminous (crustal-derived S-type granitoids) signature before ~300 Myr and after ~200 Myr (**Fig. 2d** and **SI Fig. 11d**). In addition, a recent global compilation of zircon isotopic data shows that continental crust reworking decreases from ~600 to ~225 Myr (**Fig. 1c**), during a period of gradually higher net crustal growth rate (Dhuime et al., 2012) . Subsequently, the crustal reworking rate increases, the shift correlating with the breakup of Pangea. The major tectono-magmatic trend captured by our dataset over the aggregation and dispersal of Pangea gives reasonable confidence that it is representative of exposed magmatic systems through time with minimum sampling bias.

In the continental record, the Ti-content in clinoamphibole, the Ca-content of plagioclase, the Mg-content of pyroxene and the Mg-content of olivine (e.g. those equilibrated with liquid) show an evolution from ~600 Myr ago involving an increase then a decrease to present (**Fig. 2a,b**). The compositional peaks are diachronous, being reached at 325 ± 25 Myr (Ti-content in clinoamphibole), ~225 Myr (Mg-content of pyroxene and the Ca-content of plagioclase), and ~125 Myr (Mg-content of olivine). Not surprisingly, crystallization temperatures shows a similar trend for pyroxene, amphibole and plagioclase with increasing crystallization temperatures of ~150 ºC from ~600 to ~225 Myr, and decreasing temperature since ~225 Myr in both the continental and oceanic records (**Fig. 2c** and **SI Fig. 13**). Interestingly, the thermal peak of olivine is preceded by a high-temperature plateau evolution, over a duration of ~100 Myr, overlapping with the thermal peak of pyroxene and plagioclase (**Fig. 2a and 2c**). The olivine- and glass-based thermometers (Putirka, 2008) yield information on mantle-derived primary magma compositions and mantle potential temperatures (see **Method, section 3** in the supplementary material). We observe a progressive temperature decrease of ~100 ºC since ~125 Myr that correlates, in the continental record, with a decrease in MgO-content in olivine and their host rocks (**Fig. 2a**). Consistent Tp estimates have been obtained using the PRIMELT3 MEGA software (Herzberg and Asimow, 2015) (**Fig. 2c** and **SI Fig. 14 to 17**).

DISCUSSION

Figure 2 shows that the maxima in composition and the maxima in crystallization temperatures for minerals in continental to oceanic rift magmatic systems are reached between the final stages of Pangea assembly (~325 Myr), and the final stage of its dispersal (~125 Myr). On a plate scale, warming by up to ~150 ºC of magmatic systems during Pangea aggregation is predicted by convection numerical models (Gurnis, 1988; Phillips and Bunge, 2005; Coltice et al, 2007). Therefore, we interpret the peaks magmatic temperatures between ~325 and 125 Myr, including the maximum temperature of primary magmas (*Tp*) derived from continental basalts, as the consequence of a mantle warming climax following Pangea assembling phase (**Fig. 3a)**. During the same period, the rate of crustal reworking reached its minima (**Fig. 1c**) as the internal orogens stitching Pangea's continental crust ceased to operate (Collins et al., 2011**)**, and magmatic systems became dominantly tholeiitic and metaluminous (**Fig. 2d**) as subduction zones decreased in numbers. During Pangea dispersal, from ~200 to ~125 Myr ago, Pangea blocks moved away from each other. We propose that the associated shortening of the flow wavelength (e.g. Grigné et al., 2005) and the lateral advection of cooler oceanic asthenosphere underneath continental blocks (Farrington et al., 2010) explain the cooler mantle magmatic systems observed in continental areas (**Fig. 2c**). This temperature evolution correlates with the observed change in the geochemistry of magmas as shown by the switch from dominantly tholeiitic magmatic systems when Pangea was stable (~300 to 200 Myr, **Fig. 3a**) to dominantly calc-alkaline during its dispersal as subduction zones became more prominent (**Fig. 3b**). This is consistent with the switch towards increasing crustal reworking (**Fig. 1c**) which has been emphasized in recent studies (e.g. Dhuime et al., 2012), as well as the reworking of the SCLM in orogenic systems (i.e the Circum-Pacific accretionnary orogens, Collins et al., 2011).

The evolution of magmatic temperature at crustal, mantle lithosphere and asthenosphere levels follow similar trends with a ~200 Myr offset between the onset of crustal cooling (~325 Myr, purple curve in **Fig. 3c**), and the onset of the cooling of convective mantle (~125 Myr, green curve in **Fig. 3c**). Aggregation of Pangea between 450 and 275 Myr (Veevers, 2004) led to a network of orogenic belts (Collins et al., 2011). Towards the end of this orogenic cycle, crustal thickening, radiogenic heating and mafic magma underplating (Lyubetskaya and Ague, 2010) led to a peak in magmatic temperature at crustal level, associated locally with crustal anataxis and the formation of migmatites (Augier et al., 2015) (**Fig. 3c**). From ~300 Myr onwards, orogenic crusts recovered a normal thickness via gravitational collapse and the average crustal geotherm became progressively cooler. In the lithospheric mantle, the warming preceding the peak magmatic temperature may be linked to warming in the orogenic crusts above as well as warming of the convective mantle underneath. The peak magmatic temperature in the lithospheric mantle (bracketed by the yellow trend for the upper lithospheric mantle, and blue curve for the lithosphere-asthenosphere boundary) was likely reached at 250±25 Myr. This delay can be explained by thermal inertia and the diffusion time required for the hotter potential temperature of the convective mantle to propagate through the overlying lithospheric mantle. The peak magmatic temperature in the convective mantle underneath Pangea lasted from ~225 until ~125 Myr when the major step of Pangea breakup and dispersal occurred in the Albian times (Veevers, 2004) (i.e. opening of the South Atlantic ocean (**Fig. 3b).**

IMPLICATIONS

The global change of magma compositions and fluxes between the lithosphere and outer envelopes of the planet have a potentially fascinating connection with the evolution of the oxidation and temperature state of the atmosphere and ocean through the Earth's history. Indeed, increasing magma temperature may first lead to an increased drawdown of atmospheric oxygen. Sulfur degassing has been shown to be more efficient at high magma temperatures (Scaillet et al., 1998), and sulfur is an important participant in oxygen drawdown (through formation of SO_4^{2-} compounds). Massive degassing of cooler calc-alkaline magmas is thus likely to reduce the sink for oxygen (Kump & Barley, 2007) and consequently drive or amplify a decrease in global temperatures at the surface of the planet (Royer et al., 2004).

Other broader feedbacks between the chemical record of magmas and climate change (Schmidt et al., 2015) in the last ~300 Myrs remain to be explored, acknowledging that the more calc-alkaline composition of magmas, the more explosive the activity of these volcanoes, placing more dust in the stratosphere, thereby cooling the Earth. The coupling between the inner and outer envelops of the Earth through magma activity is particularly relevant for better assessing the origins of Global Cooling of the planet since ~250 Myrs (Royer et al., 2004), following the "Great Dying" Permian Mass Extinction (Raup & Sepkoski, 1982) caused by the Siberian Trap LIPs (Burgess and Bowring, 2015). Overall, our results have profound implications on the biosphere-hydrosphere-geosphere interactions in the Earth history (McKenzie et al., 2016).

Acknowledgments

The project was supported by IRD and INSU-CNRS research funds. Keith Putirka, Richard Ernst and three anonymous reviewers are warmly thanked for their stimulating reviews and for the wonderfully spirited exchange of ideas (in sometimes mutual skepticism) surrounding data interpretation. Comments by Blair Schoene and an anonymous reviewer on an early draft

(DOI will not work until issue is live.) DOI: http://dx.doi.org/10.2138/am-2016-5868

of this paper are gratefully acknowledged. They are thanked for providing helpful comments and suggestions. Final thanks go to H. McFarlane and I. Swainson for their great editing work on the manuscript.

Author contribution

J.G. conceived the study and wrote the paper. X.F. contributed to the database building. P.R helped generate the research idea with J.G. and contributed to the writing and focusing of the paper. V.D.A. developed the Matlab scripts.

Author information

Correspondence and requests for materials should be addressed to J.G. (jerome.ganne@ird.fr)

REFERENCES

Anderson, D.L. (1982) Hotspots, polar wander, Mesozoic convection and the geoid. Nature, 297, 391–393.

Augier, R., Choulet, F., Faure, M., and Turrilot, P. (2015) A turning-point in the evolution of the Variscan orogen: the ~325 Ma regional partial-melting event of the coastal South Armorican domain (South Brittany and Vendée, France). Bulletin Société Géologique France, 186, 63-91.

Bachmann, O. (2016) Silicic Magma Reservoirs in the Earth's Crust. American Mineralogist (in press).

Bunge, H.-P. (2005). Low plume excess temperature and high core heat flux inferred from non-adiabatic geotherms in internally heated mantle circulation models. Physics of The Earth and Planetary Interiors, 153, 3-10.

Burgess, S.D. and Bowring, S.A. (2015) High-precision geochronology confirms voluminous magmatism before, during, and after Earth's most severe extinction. Science Advances, 1 (7) DOI: 10.1126/sciadv.1500470.

Chiaradia, M. (2014) Copper enrichment in arc magmas controlled by overriding plate thickness. Nature Geoscience, 7, 43–46 .

Collins, W.J., Belousova, E.A., Kemp, A.I.S., and Murphy, J.B. (2011) Two contrasting Phanerozoic orogenic systems revealed by hafnium isotope data. Nature Geoscience, 4, 334-337.

Coltice, N., Bertrand, H., Rey, P., Jourdan, F., Phillips, B.R., and Ricard, Y. (2009) Global warming of the mantle beneath continents back to the Archaean. Gondwana Research, 15, 254–266.

Coltice, N., Phillips, B.R., Bertrand, H., Ricard, Y. and. Rey, P. (2007) Global warming of the mantle at the origin of flood basalts over supercontinents. Geology, 35, 391-394.

Courtillot, V., Jaupart, C., Manighetti, I., Tapponnier, P., and Besse, J. (1999). On causal links between flood basalts and continental breakup. Earth and Planetary Science Letters, 166, 177–195.

Dhuime, B., Hawkesworth, C.J., Cawood, P.A., Storey, C.D. (2012) A Change in the Geodynamics of Continental Growth 3 Billion Years Ago. Science, 335, 1334-1336.

Ernst, R.E. and Buchan, K.L. (1997) Giant radiating dyke swarms: their use in identifying pre-Mesozoic large igneous provinces and mantle plumes. AGU Geophysical Monograph, 100, 297-333.

Ernst, R.E. (2014) Large Igneous Provinces. Cambridge University Press 653 p.

Farrington, R.J., Stegman, D.R., Moresi, L.N. Sandiford, M., and May, D.A. (2010) Interactions of 3D mantle flow and continental lithosphere near passive margins. Tectonophysics, 483, 20-28.

Ghiorso, M.S., and Sack, R.O. (1995) Chemical mass-transfer in magmatic processes IV. A revised and internally consistent thermodynamic model for the interpolation and extrapolation of liquid–solid equilibria in magmatic systems at elevated temperatures and pressures. Contribution to Mineralogy and Petrology, 119, 197-212.

Grigné C., Labrosse S., and Tackley P.J. (2005) Convective heat transfer as a function of wavelength: Implications for the cooling of the Earth. Journal of Geophysical Research, 110, B03409, doi:10.1029/2004JB003376.

Grove, T.L., and Baker, M.B. (1984) Phase equilibrium control on the tholeiitic versus calc-alkaline differentiation trends. Journal of Geophysical Research, 89, 3253–3274.

Gurnis, M. (1988) Large-scale mantle convection and the aggregation and dispersal of supercontinents. Nature, 332, 695–699.

Herzberg, C. (2011) Basalts as temperature probes of Earth's mantle. Geology, 39, 1179-1180.

Herzberg, C., and Asimow, P.D. (2015). PRIMELT3 MEGA.XLSM software for primary magma calculation: Peridotite primary magma MgO contents from the liquidus to the solidus. Geochemistry Geophysics Geosystems, 16, doi: 10.1002/2014GC005631.

Hill, R.I. (1991) Starting plumes and continental break-up. Earth and Planetary Science Letters, 104, 398–416.

Hole, M.J. (2015) The generation of continental flood basalts by decompression melting of internally heated mantle. Geology, 43, 311–314.

Keller, C.B. and Schoene, B. (2012) Statistical geochemistry reveals disruption in secular lithospheric evolution about 2.5 Gyr ago. Nature, 485, 490–493.

Kump, L. R. and Barley, M. E. (2007) Increased subaerial volcanism and the rise of atmospheric oxygen 2.5 billion years ago. Nature, 448, 1033-1036.

Labrosse, S., and Jaupart, C. (2007) Thermal evolution of the Earth: secular changes and fluctuations of plate characteristics. Earth and Planetary Science Letters, 260, 465–481.

Lenardic, A., Moresi, L., Jellinek, A. M., O'Neill, C. J., Cooper, C. M. and Lee, C.-T. A. (2011) Continents, supercontinents, mantle thermal mixing, and mantle thermal isolation: Theory, numerical simulations, and laboratory experiments. Geochemistry Geophysics Geosystems, 12, doi:10.1029/2011gc003663 .

Lyubetskaya, T., and Ague, J.J. (2010) Modeling metamorphism in collisional orogens intruded by magmas: II. Fluid flow and implications for Barrovian and Buchan metamorphism, Scotland. American Journal of Science, 310, 459-491.

McKenzie D., and Bickle M.J. (1988). The volume and composition of melt generated by extension of the lithosphere. Journal of Petrology, 29, 625–679.

McKenzie N. R., Horton, B. K., Loomis, S. E., Stockli, D. F., Planavsky, N. J., and Lee, C.-T. A. (2016) Continental arc volcanism as the principal driver of icehouse-greenhouse variability. Science, 352 (6284): 444 DOI: 10.1126/science.aad5787.

Phillips, B, R., and Bunge, H.P. (2005). Heterogeneity and time dependence in 3D spherical mantle convection models with continental drift. Earth and Planetary Science Letters, 233, 121-135.

Putirka, K. D. (2005) Igneous thermometers and barometers based on plagioclase + liquid equilibria: Test of some existing models and new calibrations. American Mineralogist, 90, 336–346.

Putirka, K. D. (2008) Thermometers and barometers for volcanic systems, in: Putirka, K. D., and Tepley, F. eds., Reviews in Mineralogy and Geochemistry, 69, 61-120.

Putirka, K. D. (2016) Rates and styles of planetary cooling on Earth, Moon, Mars, and Vesta, using new models for oxygen fugacity, ferric-ferrous ratios, olivine-liquid Fe-Mg exchange, and mantle potential temperature. American Mineralogist, 101,819-840.

Raup D. M., and Sepkoski J.J. (1982). Mass extinctions in the marine fossil record. Science, 215, 1501–1503.

Royer, D.L., Berner, R.A., Montañez, I.P., Tabor, N.J., and Beerling, D.J. (2004) CO_2 as a primary driver of Phanerozoic climate change. GSA Today, 14, 4-10.

Rey P.F. (2015) The Geodynamic of mantle melting. Geology, 43, 367-368.

Ridolfi, F. and Renzulli, A. (2012) Calcic amphiboles in calc-alkaline and alkaline magmas: thermobarometric and chemometric empirical equations valid up to 1,130°C and 2.2 GPa. Contribution to Mineralogy and Petrology, 163, 877–895.

Scaillet, B., Clémente, B., Evans, B. W., and Pichavant, M. (1998) Redox control of sulfur degassing in silicic magmas. Journal of Geophysical Research: Solid Earth, 103, 23937-23949.

Schmidt, A., Kirsten, E.F., and Elkins-Tanton, L.T. (2015) Volcanism and Global Environmental Change (Cambridge Univ.Press, Cambridge, UK).

Shabani, A.A.T, Lalonde, E., and Whalen, J.B. (2003) Composition of biotite from granitic rocks of the Canadian Appalachian Orogen : A potential tectonomagmatic indicator ?. Canadian Mineralogist, 41, 1381 – 1396.

Smith, D.J. (2014). Clinopyroxene precursors to amphibole sponge in arc crust. Nature Communications, 5, 4329.

Veevers, J.J. (2004) Gondwanaland from 650–500 Ma assembly through 320 Ma mergers in Pangea to 185–100 Ma breakup: supercontinental tectonics via stratigraphy and radiometric dating. Earth-Science Reviews, 68, 1-132.

Villiger, S., Ulmer, P. and Muntener, O. (2007) Equilibrium and fractional crystallization experiments at 0·7 GPa; the effect of pressure on phase relations and liquid compositions of tholeiitic magmas. Journal of Petrology, 48, 159-184.

Whitaker, M. L., Nekvasil, H., Lindsley D. H., and Difrancesco, N. J. (2007) The Role of Pressure in Producing Compositional Diversity in Intraplate Basaltic Magmas. Journal of Petrology, 48, 365-393.

Yale, L.B., and Carpenter, S.J. (1998). Large igneous provinces and giant dike swarms: proxies for supercontinent cyclicity and mantle convection. Earth and Planetary Science Letters, 163, 109–122.

Zen, E-an. (1986). Aluminum Enrichment in Silicate Melts by Fractional Crystallization: Some Mineralogic and Petrographic Constraints. Journal of Petrology, 27, 1095-1117.

FIGURES CAPTIONS

Figure 1. Chemical record of magmas through times. (a) Phase diagram, contoured for MgO, of mantle melting (after Herzberg and Asimow, 2015; modified). Mantle melting at the solidus (blue and red stars) for contrasting potential temperatures (blue and red circles) leads to contrasting MgO content in primary magmas. During their ascent to the surface (black arrows) these primary magmas are modified by (often fluid-induced) fractional crystallization in the lithosphere and by crustal assimilation (Grove and Baker, 1984), forming calc-alkaline series in which the mineralogical composition depends on the depth of crystallization. The less modified magmas (tholeiitic affinity) keep the memory of the potential temperature. The colored bars in (a), which are labeled by mineral type. are not precisely constrained by temperature data. (b) Intracontinental, arc and oceanic magmatic systems through time. Oceanic magmatic systems and magmatic systems at continental margins are increasing during Pangea dispersal from ~175 Myr onwards. (c) Peak production of tholeiitic magmas (TH index : more $Fe_2O_{3\ total}$-enriched at MgO ~4-6 wt%; Chiaradia, 2014) and minimum crustal reworking (yellow curve, from Dhuime et al., 2012) are reached during Pangea stability phase.

Figure 2. Chemical record of magmatic minerals. (a) Temperatures of crystallization through times based on magmatic olivines from continental settings (red points) and evolution of Mg-content of olivines and their host rocks. (b) Chemical evolution of pyroxenes, plagioclases and clinoamphiboles. (c) Crystallization temperature of magmatic minerals (open grey circles) obtained with different thermometers (Putirka, 2008; Ridolfi and Renzulli, 2012). Statistical assessment of their averaged evolution through time is given by the colored drawbars. From ~200 Myr onwards, the increasing occurrence of lower magmatic

temperatures for pyroxenes and plagioclases point toward increasing fractionation of magmas at progressively deeper levels in a progressively cooler continental lithosphere. Mantle potential temperature (*Tp*) is calculated with the Ol-Liq. thermometer (green points), using a melt fraction of 0.15. (a) Samples of basalts have been re-analysed using PRIMELT3 MEGA (Herzberg and Asimow, 2015) software to obtain complementary Tp estimates (red points ; see **Method, section 3** in the supplementary material). (d) Correlation between the occurrence of Al-rich biotite and the Aluminium Saturation Index (ASI) of magmas defined as the molar ratio Al_2O_3 / (CaO + K_2O + Na_2O) (Zen, 1986). Numbers in the middle of the purple curve correspond to the ASI values.

Figure 3. Supercontinent cycle and thermal regime. (a, b) Sketches illustrating plate and mantle dynamics and climate (Farrington et al., 2010) during amalgamation and breakup of the Pangea supercontinent. Paleogeographic configurations are based on a Triassic and Cretaceous reconstruction (Veevers, 2004). The external (circum-Pacific) system comprises a number of discrete orogens that, together, have probably existed for 550 Myr (Collins et al., 2011). (c) Thermal peaks for magmatic pyroxenes and plagioclases (~225 Myr), dominantly tapping (or considered to reflect conditions in) the sub-continental lithospheric mantle, span a period of orogenic collapse for the belts suturing the Pangea supercontinent. Thermal peak for olivines (~125 Myr), dominantly tapping the sub-continental asthenospheric mantle, corresponds to a period of enhanced supercontinent breakup. The green, blue and yellow curves come from **Fig. 2** ; the shape of the purple curve "metamorphic record" is not constrained by temperature data.

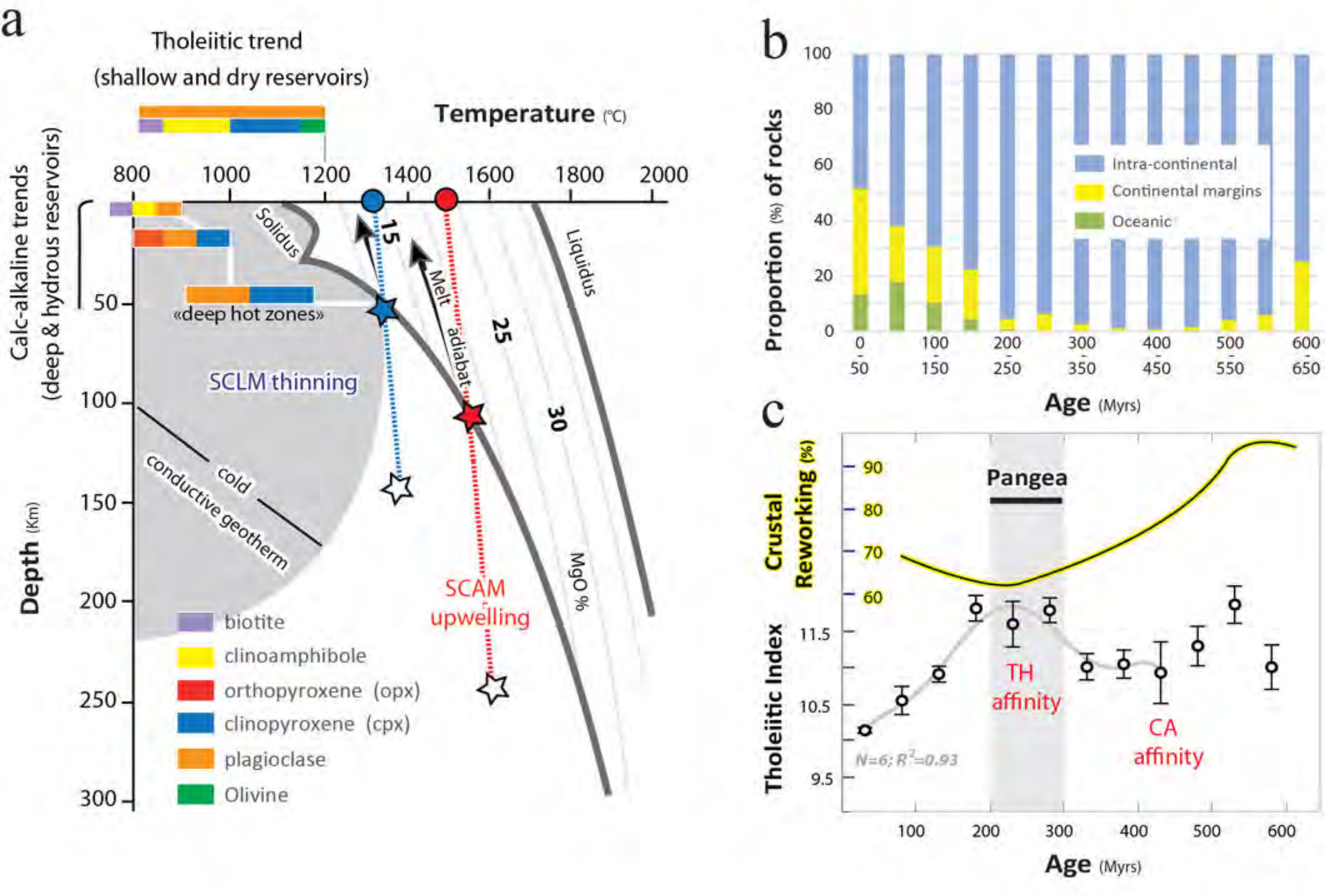
a
Tholeiitic trend
(shallow and dry reservoirs)
Temperature (°C)
800 1000 1200 1400 1600 1800 2000
Calc-alkaline trends
(deep & hydrous reservoirs)
Solidus
Liquidus
15
Melt adiabat
25
30
«deep hot zones»
SCLM thinning
cold conductive geotherm
SCAM upwelling
MgO %
Depth (Km)
50
100
150
200
250
300
biotite
clinoamphibole
orthopyroxene (opx)
clinopyroxene (cpx)
plagioclase
Olivine
b
Proportion (%) of rocks
Intra-continental
Continental margins
Oceanic
Age (Myrs)
c
Crustal Reworking (%)
Pangea
Tholeiitic Index
TH affinity
CA affinity
N=6; R²=0.93
Age (Myrs)

Figure 1

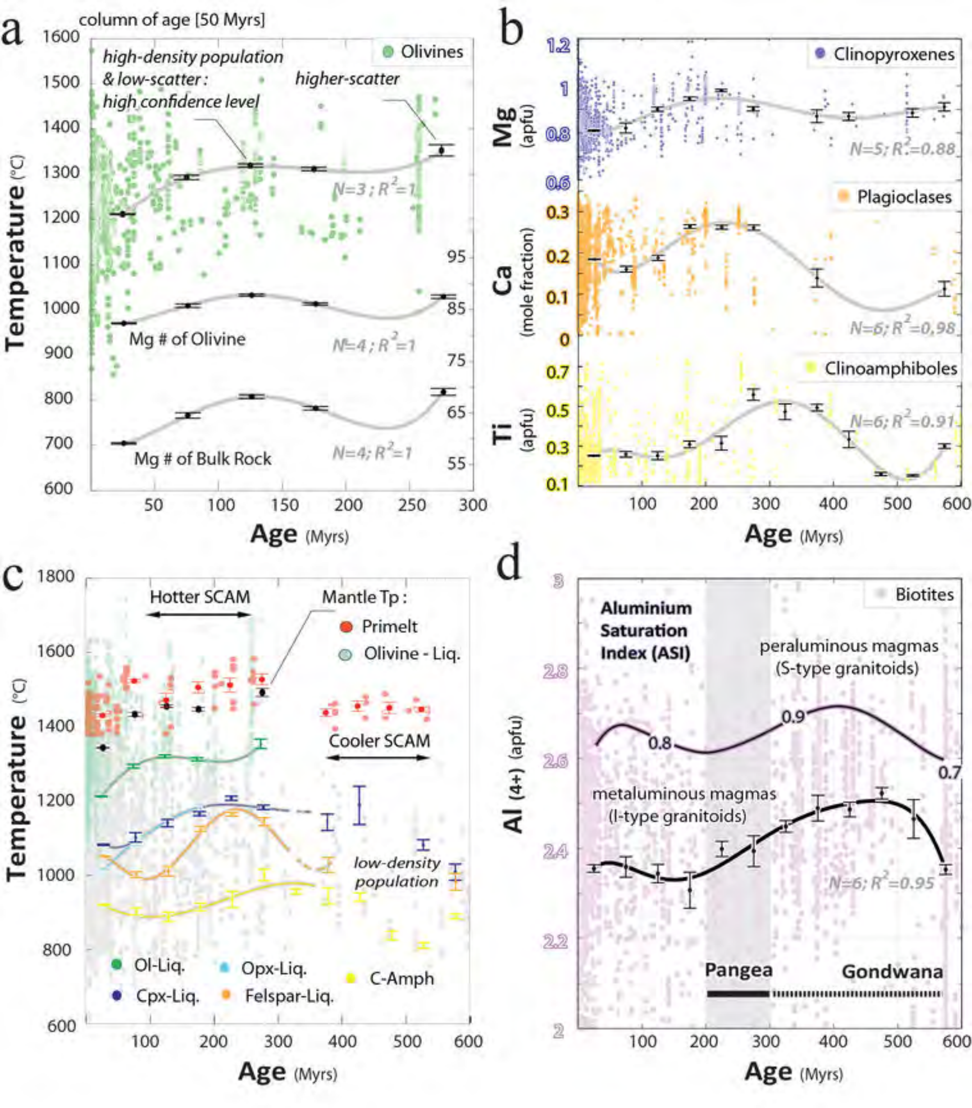

a
column of age [50 Myrs]
high-density population
& low-scatter :
high confidence level
higher-scatter
Olivines
Temperature (°C)
N=3 ; R²=1
Mg # of Olivine
N=4 ; R²=1
Mg # of Bulk Rock
N=4; R²=1
Age (Myrs)
b
Clinopyroxenes
Mg (apfu)
N=5; R²=0.88
Plagioclases
Ca (mole fraction)
N=6; R²=0,98
Clinoamphiboles
Ti (apfu)
N=6; R²=0.91
Age (Myrs)
c
Hotter SCAM
Mantle Tp :
Primelt
Olivine - Liq.
Cooler SCAM
low-density
population
Temperature (°C)
Ol-Liq.
Opx-Liq.
C-Amph
Cpx-Liq.
Felspar-Liq.
Age (Myrs)
d
Biotites
Aluminium
Saturation
Index (ASI)
peraluminous magmas
(S-type granitoids)
0.8
0.9
0.7
metaluminous magmas
(I-type granitoids)
N=6; R²=0.95
Al (4+) (apfu)
Pangea
Gondwana
Age (Myrs)

Figure 2

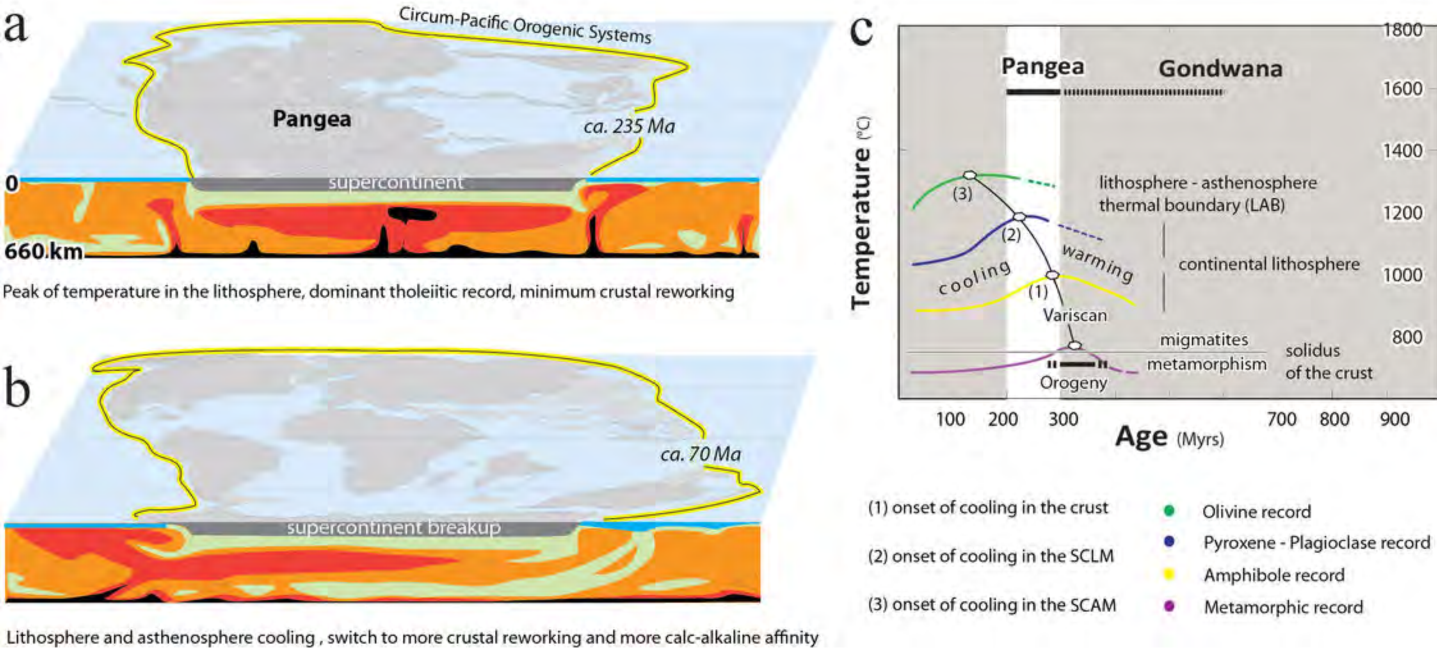
a
Circum-Pacific Orogenic Systems
Pangea
ca. 235 Ma
0
supercontinent
660 km
Peak of temperature in the lithosphere, dominant tholeiitic record, minimum crustal reworking
b
ca. 70 Ma
supercontinent breakup
Lithosphere and asthenosphere cooling , switch to more crustal reworking and more calc-alkaline affinity
c
Pangea
Gondwana
1800
1600
1400
1200
1000
800
Temperature (°C)
lithosphere - asthenosphere
thermal boundary (LAB)
continental lithosphere
(3)
(2)
(1)
cooling
warming
Variscan
migmatites
metamorphism
solidus
of the crust
Orogeny
100
200
300
700
800
900
Age (Myrs)
(1) onset of cooling in the crust
(2) onset of cooling in the SCLM
(3) onset of cooling in the SCAM
Olivine record
Pyroxene - Plagioclase record
Amphibole record
Metamorphic record

Figure 3